Supplemental Figure Legends:

Figure S1: Cell cycle after 24 hours of CDK inhibitor treatment. (**A**) Dose-response curves to various CDK inhibitors, and (**B**) representative cell cycle dot-plots. Cells were treated for 24 hours at the indicated dose prior to 15 minutes BrdU pulse, cell harvesting, fixation, staining, and analysis by flow cytometry.

Figure S2: In vitro protection from genotoxic agents using PQ. (**A**) Quantification of mean nuclear intensity from γH2AX immunofluorescence images (Figure 1A) with and without 6 Gy IR at 0 and 3 hours after exposure with PD0332991. N=139 or greater for each condition; box = middle 50%, whiskers = 0-25% and 75-100%. Significance determined by Kruskal-Wallis ($p<0.0001$) with Dunn post-hoc test for pair-wise comparisons. (**B**) Flow cytometry analysis of γH2AX formation after 2BrIC and doxorubicin treatment in tHDFs. (**C**) Comet tail area with 24 hours in 1 μM 2BrIC prior to indicated IR dose. 40 cells in each condition were imaged at 10x magnification. (**D**) Quantification of P53-Ser15-phosphorylation from western blots (Figure 1B) normalized to actin after PD0332991 treatment and 6 Gy IR exposure. (**E**) Ratios of colony formation per cell in clonogenic assays after IR with or without PD0332991 in A2058 and tHDF. *$p<0.01$, **$p<0.0001$ for pair-wise comparisons.

Figure S3: In vitro protection from doxorubicin using PQ. (**A**) Quantification of WST assay in tHDFs, WM2664, and A2058 cell lines 1 week after the treatment schedules from Figure 2A using 2BrIC and 1 μM doxorubicin. Other CDK4/6 inhibitors (**B**) flavopiridol, (**C**) roscovitine, and (**D**) R547 were assessed for their ability to protect from doxorubicin exposure using CellTiter Glo assay. For (**B**), (**C**), and (**D**), doxorubicin concentrations were 122 nM for A2058 and WM2664, and 370 nM for tHDF. #$p<0.01$ vs. DMSO, ##$p<0.001$ vs. DMSO, *$p<0.01$ vs. Dox, **$p<0.001$ vs. Dox.

Figure S4: Apoptosis, viability, CAFC, and oligopotent progenitor population frequencies after CDK4/6 inhibitor treatment. (**A**) Total BM-MNC counts from mice exposed to 48 hours of CDK4/6 inhibitor treatment. Caspase3 and viability of total Lin- cells (**B**) and HSC (**C**) with and without 48 hours of PD0332991 exposure and 24 hours of BrdU pulse. (**D**) Frequency of Lin- cells of myeloid, erythroid, and lymphoid progenitors after 48 hours of CDK4/6 inhibition. (**E**) CAFC results at 1, 2, and 5 weeks after 48 hours of PD0332991 treatment and bone marrow harvest without BrdU exposure.

Figure S5: CDK4/6 inhibition induces mild, reversible myelosuppression. Daily oral gavage with PD0332991 for 12 days with complete blood counts (CBCs) at indicated time points. Data are shown as a moving average with each point representing the mean of three consecutive CBCs. Solid black bar indicates duration of PD0332991 treatment.

Figure S6: CDK4/6 inhibition improves radiation survival in different inbred strains. . (**A**) Survival of adult female C57Bl/6 mice after 8.5 Gy TBI. (**B**) Survival of adult female C57Bl/6 mice after 6.5 Gy TBI. (**C**) Survival of adult female CH3 mice after 7.5 Gy TBI. All p-values determined using the log-rank test.

Figure S7: Brief PQ at the time of TBI attenuates myelosuppression and augments count recovery after sublethal ionizing radiation. Weekly CBCs on tail vein bleeds of PD0332991 treated and untreated mice after 6.5 Gy TBI, a sub-lethal dose. Asterisk(s) indicate statistical significance determined by a 2-sided t-test.

Figure S8: Hematologic profiles are unchanged >100 days after sublethal IR exposure. Results of complete blood counts with differential at 143-242 days after 6.5 or 7.5 Gy TBI with

and without PD0332991 treatment are shown and compared to age-matched unirradiated, untreated animals. Myeloid cells = granulocytes + monocytes.

Figure S9: In vivo radioprotection of tumor-bearing mice using PQ. Bodyweights in mice with autochthonous melanomas with or without a single dose of PD0332991 at -4 hours prior to 7.5 Gy TBI. *$p<0.05$.

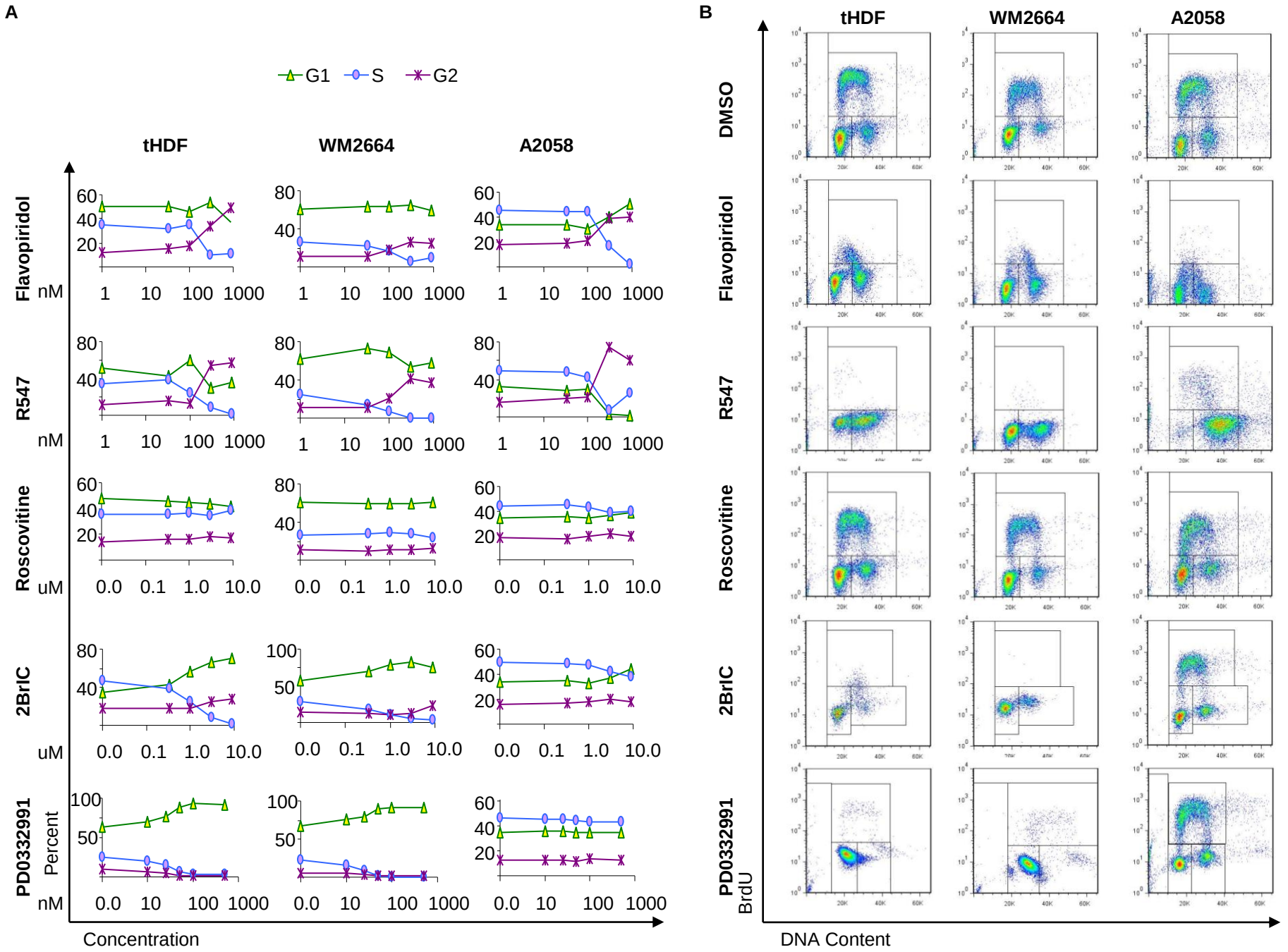

Johnson et al., Figure S1

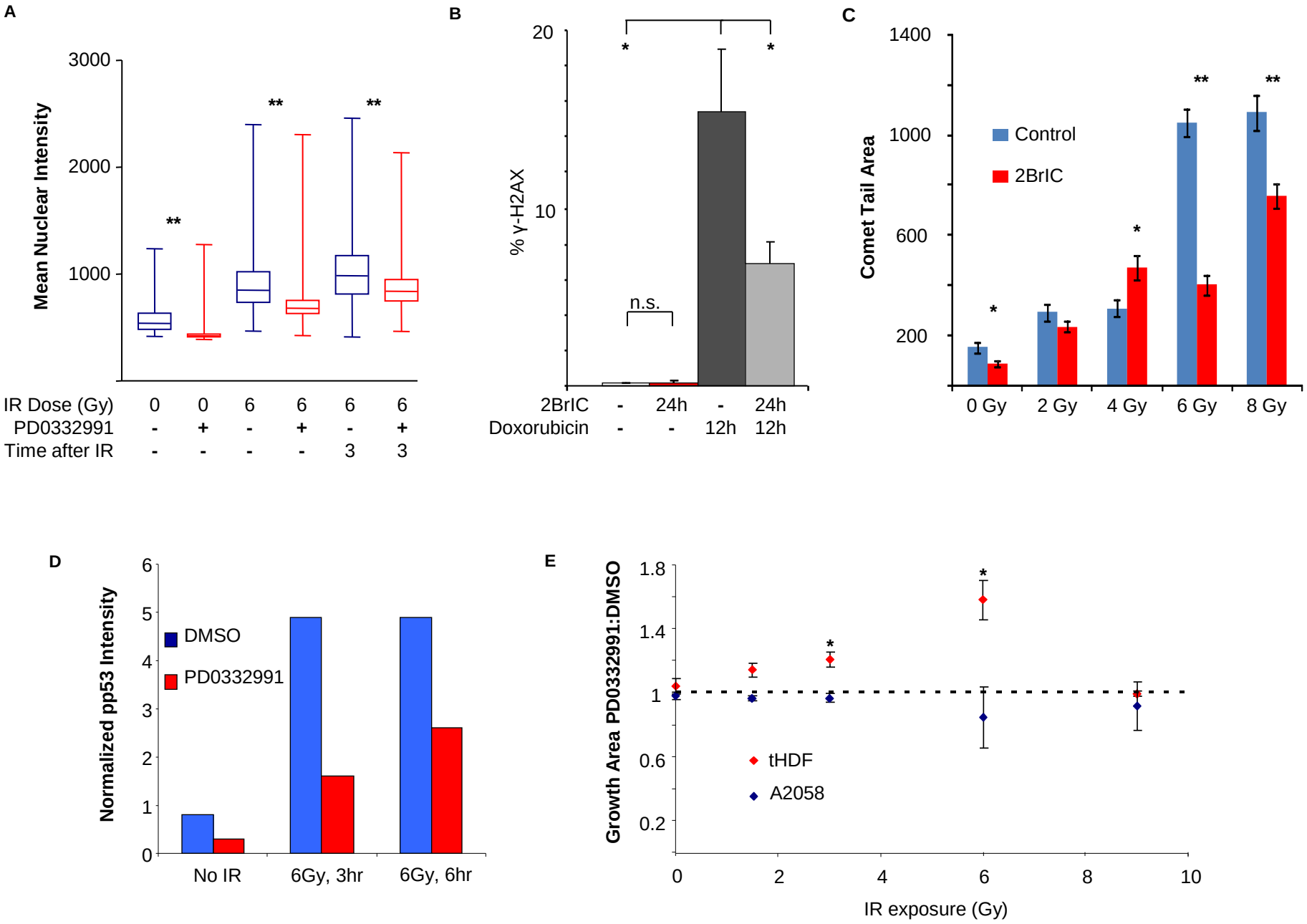

Johnson et al., Figure S2

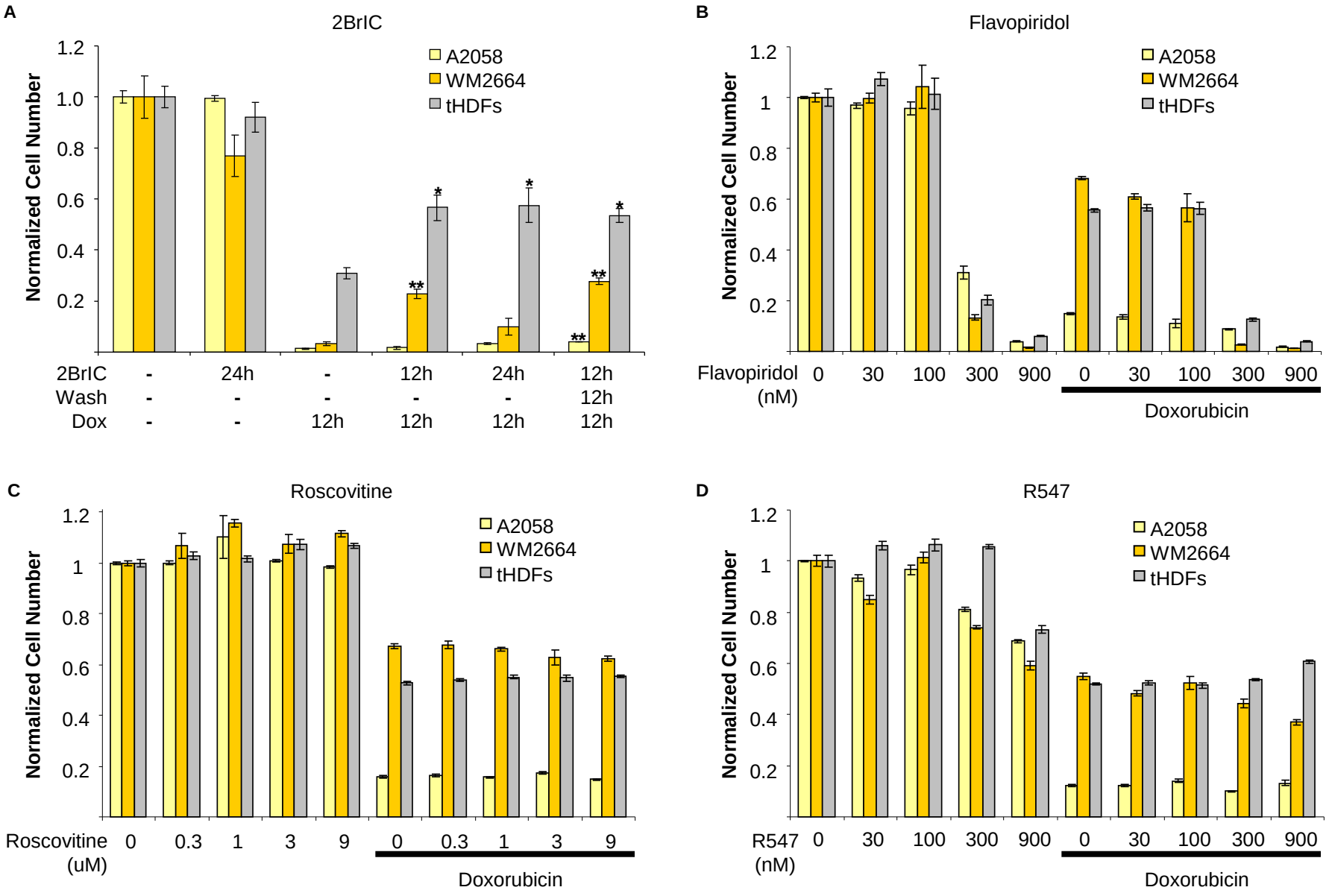

Johnson et al., Figure S3

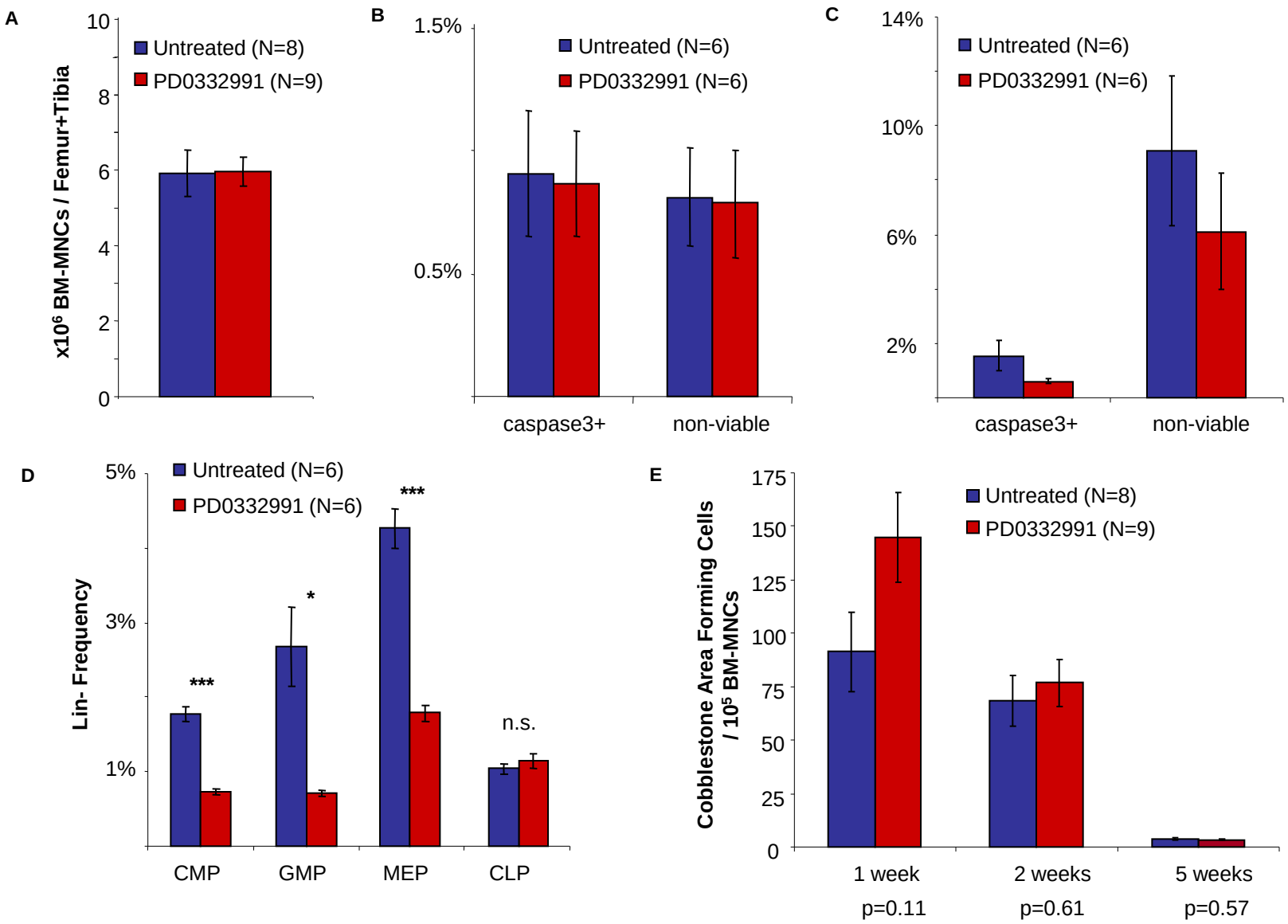

Johnson et al., Figure S4

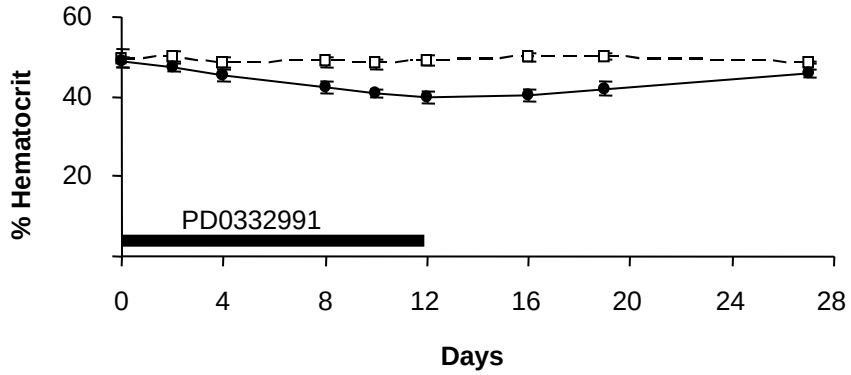

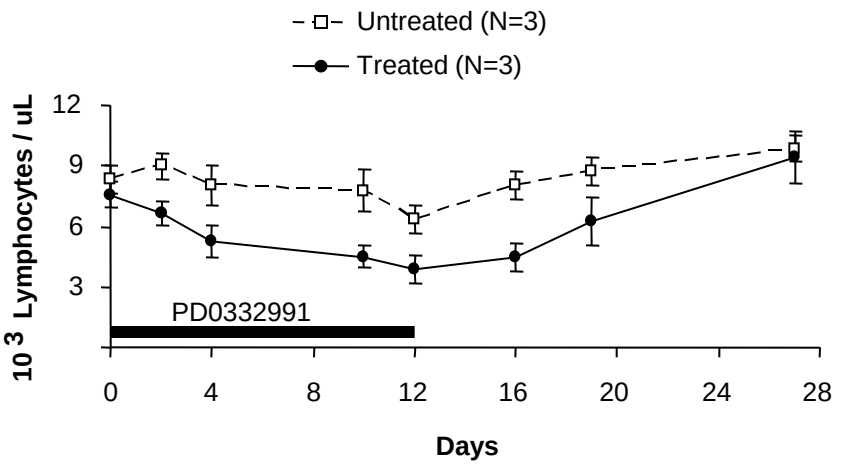

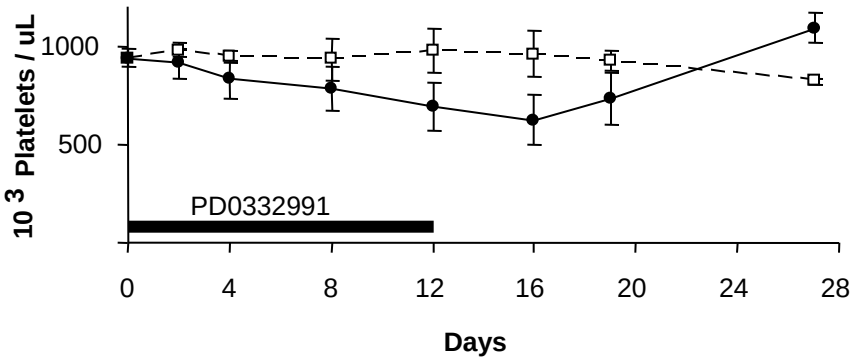

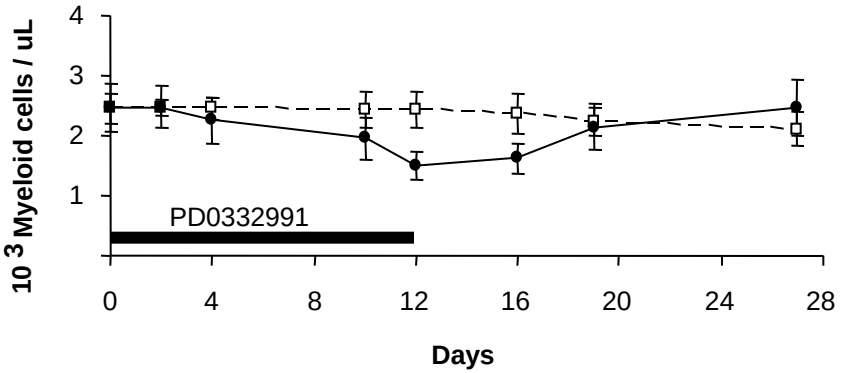

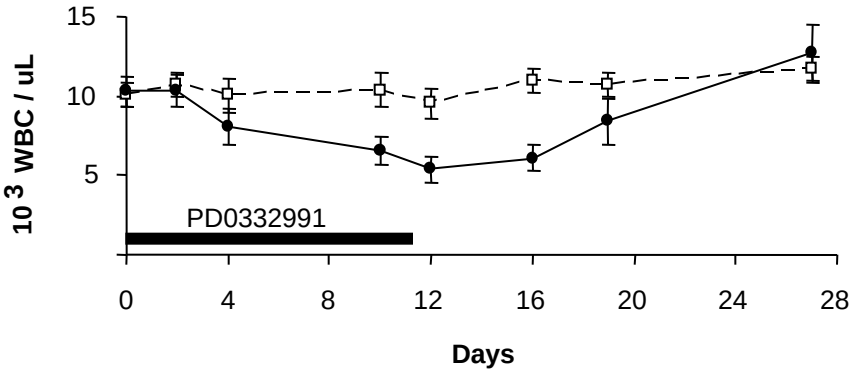

Johnson et al., Figure S5

A

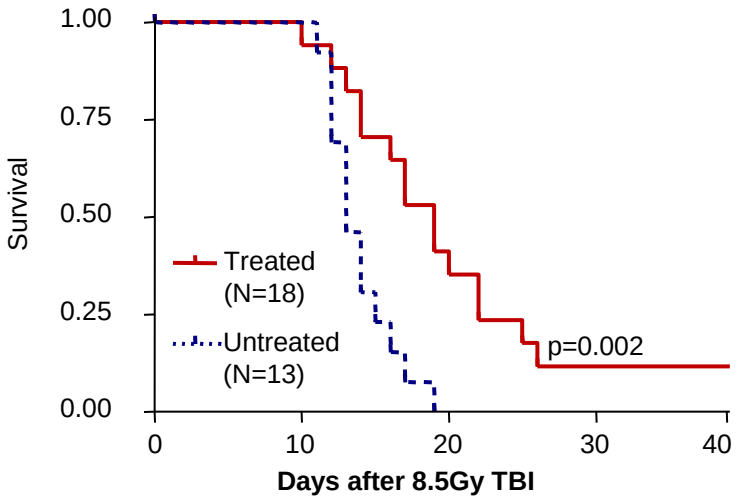

B

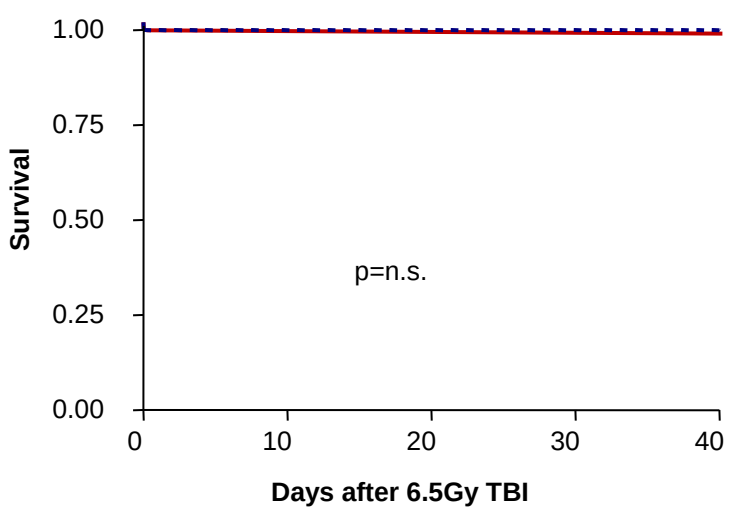

C

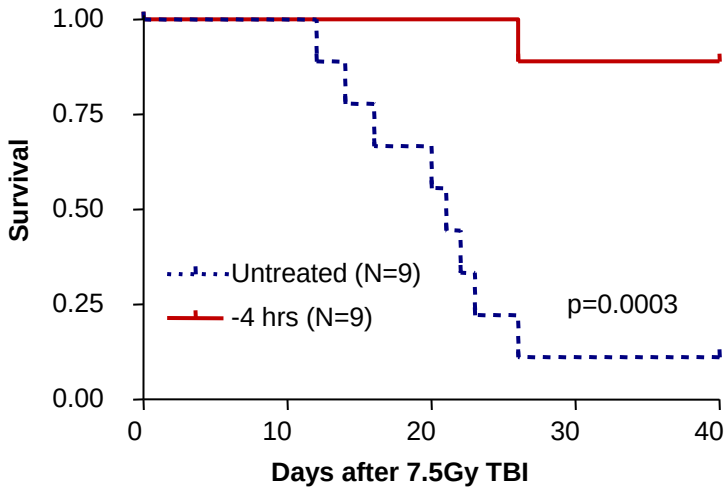

Johnson et al., Figure S6

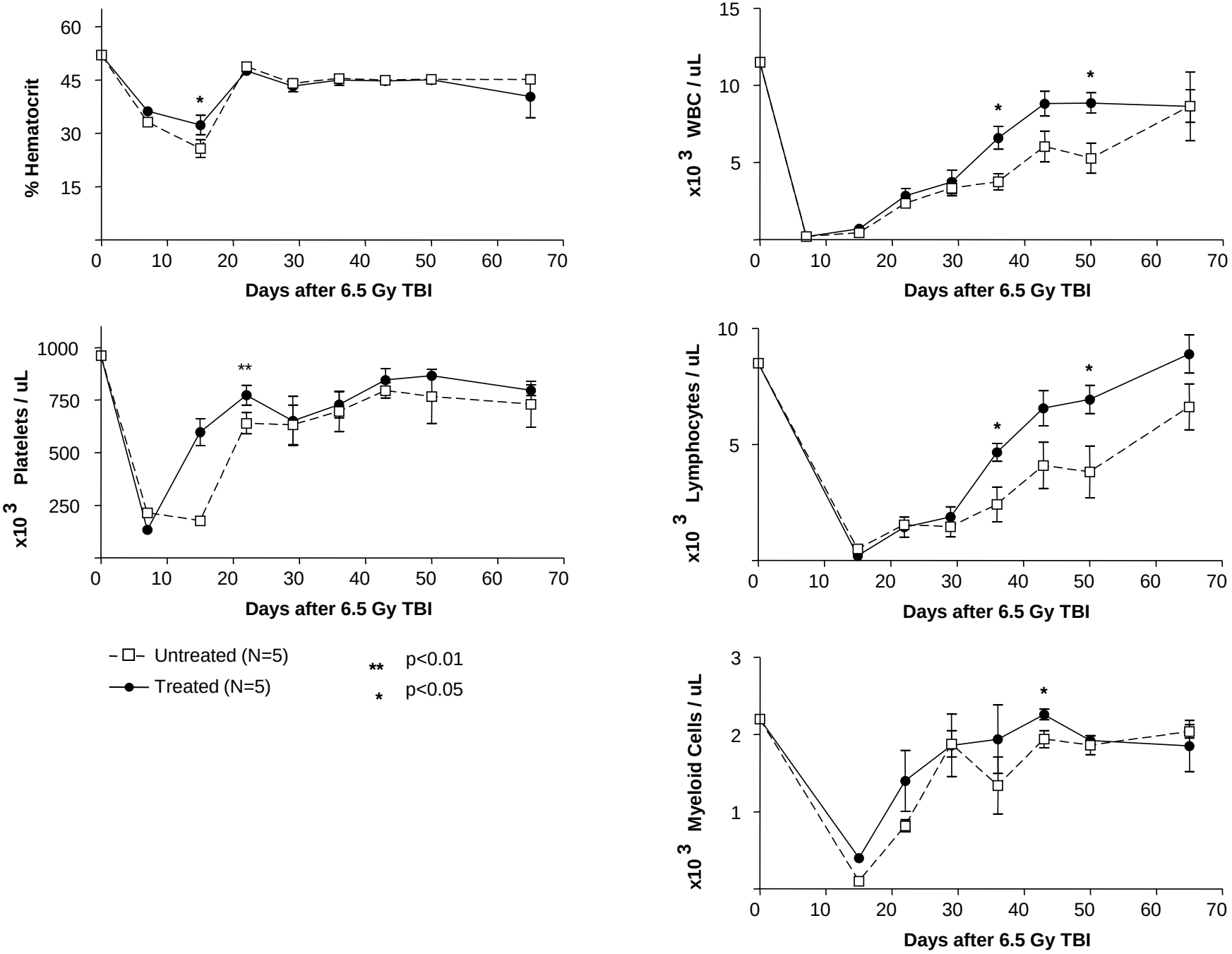

Johnson et al., Figure S7

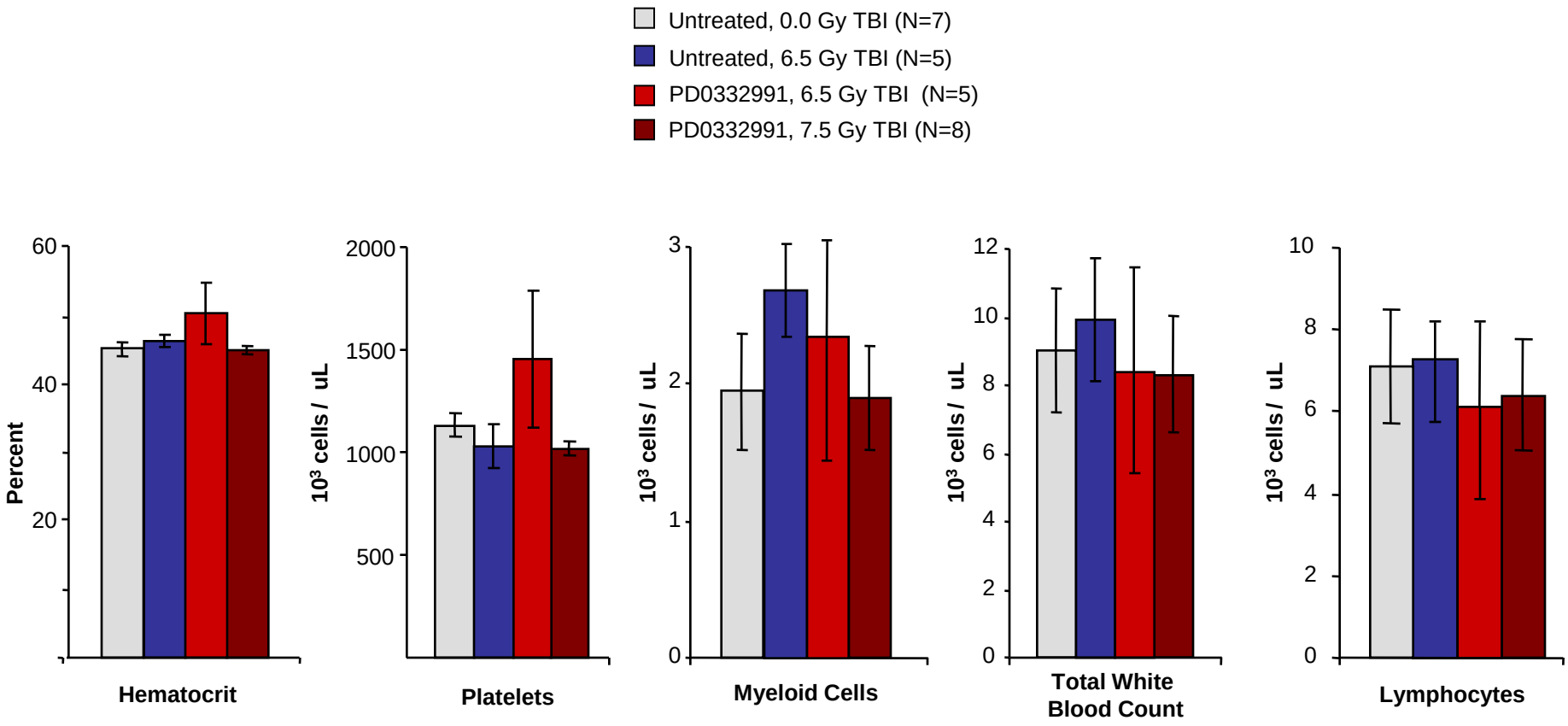

Johnson et al., Figure S8

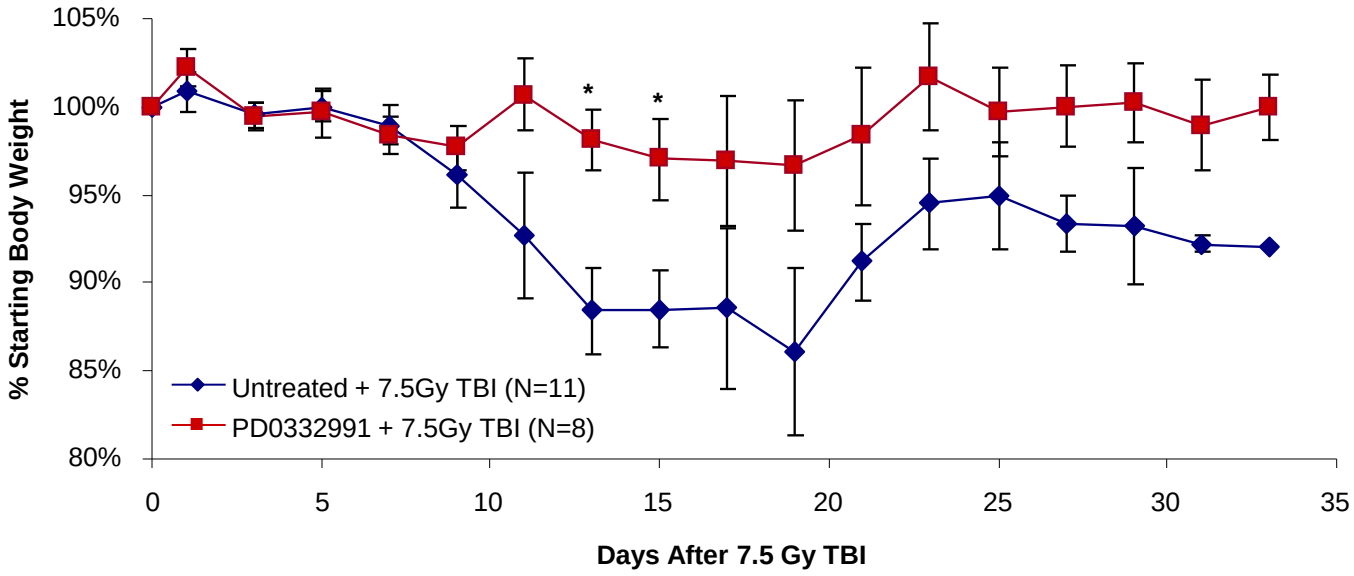

Johnson et al., Figure S9